IEEE Access
Multidisciplinary | Rapid Review | Open Access Journal

Received July 18, 2020, accepted August 31, 2020, date of publication September 7, 2020, date of current version September 18, 2020.

Digital Object Identifier 10.1109/ACCESS.2020.3022292

Analysis of Partial Discharges in Electrical Tree Growth Under Very Low Frequency (VLF) Excitation Through Pulse Sequence and Nonlinear Time Series Analysis

PABLO DONOSO[1], ROGER SCHURCH[1], (Member, IEEE), JORGE ARDILA-REY[2], (Member, IEEE), AND LUIS ORELLANA[2]

[1]Department of Electrical Engineering, Universidad Técnica Federico Santa María, Valparaíso 2390123, Chile
[2]Department of Electrical Engineering, Universidad Técnica Federico Santa María, Santiago 8940000, Chile

Corresponding author: Pablo Donoso (pablo.donoso@alumnos.usm.cl)

This work was supported in part by the Agencia Nacional de Investigacion y Desarrollo (ANID) through the Fondo Nacional de Desarrollo Científico y Tecnológico (FONDECYT) under Grant 11181177, and in part by Universidad Técnica Federico Santa María under Grant PI_L_18_19 and Grant PIIC.

ABSTRACT Electrical treeing is the main degradation mechanism in high voltage polymeric insulation, that leads to power system plant failure and the loss of electricity supply. Electrical trees grow under partial discharge (PD) activity, which can be measured and analyzed to understand and characterize electrical tree growth. In this work, PD measurements were analyzed for electrical trees grown in epoxy resin needle-plane samples under very low frequency (VLF, 0.1 Hz) voltage excitation. VLF is interesting as it is used for testing power cables and other high capacitance insulation loads. However, more experience and new methods are needed for PD interpretation. PDs were studied using two tools: pulse sequence analysis (PSA) and nonlinear time series analysis (NLTSA) from dynamic system theory. PSA was treated here as a particular case of NLTSA since their constructions are similar in their mathematical treatment. The experimental results showed that electrical trees grown at VLF had branch-type structure and times to breakdown about fifty times larger than samples aged at industrial frequency. PSA plots were compared with 2D projections of state-space trajectories that represent the dynamics of the nonlinear system (NLTSA approach). In terms of graphical representation, NLTSA 2D projections generated more clusters than the PSA plots, thus, it was interpreted that NLTSA revealed more details about the nonlinear dynamic system associated with electrical tree growth. On the other hand, using the NLTSA approach, the correlation dimension was estimated to characterize the electrical tree growth. The results showed a different evolution obtained for VLF excitation compared to the results reported for test samples aged at industrial frequency in other studies.

INDEX TERMS Electrical trees, partial discharges, pulse sequence analysis, nonlinear time series analysis, very low frequency testing, correlation dimension.

I. INTRODUCTION

Electrical trees are hollow tubes that grow in polymeric insulation under high electric field stress [1]. This phenomenon is one of the main causes of solid dielectric breakdown, and thus, it can cause catastrophic failure of electrical equipment, for example in power cables used in power grids [2], [3]. The initiation of this degradation phenomenon is generally associated with metallic or semiconducting protrusions, contaminants, discharge cavities or water trees [1]. Electrical trees grow under the action of partial discharges (PD) [4], [5], which correspond to a localized dielectric breakdown in an electrical insulation system [6]. Partial discharge activity changes during electrical treeing due to the growth itself and the diversity of physical and chemical factors involved in this complex phenomenon [4], [5], [7], [8].

Electrical tree growth is affected by the frequency of the voltage excitation that is stressing the system [9]–[13].

The associate editor coordinating the review of this manuscript and approving it for publication was Mehdi Bagheri.

This work is licensed under a Creative Commons Attribution 4.0 License. For more information, see https://creativecommons.org/licenses/by/4.0/

Nowadays, electrical components of a power grid, and thus the dielectric systems that conform them, are subjected to a variety of frequencies due to the grid operation and non-linear loads [14], or due to tests needed for commissioning and maintenance of equipment [15], [16]. Electrical treeing is normally researched in laboratory, with test samples artificially created, where tree growth is analyzed through PD measurements and imaging of electrical tree structures, as a method of obtaining a better understanding of the phenomenon [7], [17]. Polymeric materials that have been used for electrical treeing experiments include XLPE, PE and epoxy resin. Investigations have shown that the main features of treeing analysis remain similar among these materials [18]–[21]. Electrical tree growth has been mainly studied for industrial frequency, i.e. alternating current of 50-60 Hz [4], [8], [17], while the study of other excitation frequencies are gaining interest [9], [10]. One particular case is the use of very low frequency (VLF) excitation, which corresponds to an alternating voltage with frequencies between 0.01-1 Hz. This type of excitation is mostly used for testing power cables, which is recommended in standards [16], [22], and in less degree, in rotating machines [23] and other high capacitance insulation loads. In this regard, the use of VLF excitation is an interesting choice because these tests require smaller voltage sources than industrial frequency tests and it is less likely to produce harmful accumulation of space charge within the insulation, as it is the case of DC tests [22], [24], [25]. However, there are insufficient data to allow accurate interpretation of PD measurements in VLF testing [16] and new methods of PD analysis are needed for insulation condition assessment under VLF excitation [11], [26].

Studies of electrical tree propagation under VLF excitation are scarce. It is known that with frequency reduction, electrical trees grow slower and their shape is also affected. It has been reported that the time to breakdown at 0.1 Hz was three times longer than at 1 Hz [9] and trees grown at VLF (0.1 Hz) can be almost five times slower than industrial frequency (50 Hz) in test samples at the same high voltage level [11], showing that the tree growth rate is not linear with respect to the frequency. Moreover, electrical trees grown at VLF have a less bushy/dense structure compared to those grown at industrial frequencies [9], [11].

Partial discharge activity, with its erosion action, is the main cause of electrical tree propagation [1], [27]. Therefore, the analysis of PD becomes essential to the understanding of electrical tree growth. PD phenomenon is a dynamical process that involves the electrical field distribution, space charge phenomenon and electrical conductivity distribution along the tree structure, and all of this is influenced by the voltage and frequency of the excitation, among others [26], [28].

Typically, PDs have been analyzed with statistical parameters and patterns via phase-resolved partial discharge (PRPD) plots, i.e. the phase position of the PD amplitude measurement (apparent charge) with respect to the applied voltage sinusoidal waveform. However, this approach misses information concerning the temporal evolution of PD pulses [29], [30], which can be specially important when solid or liquid dielectrics are involved [31], [32]. An alternative approach is to consider the dynamic between consecutive PD pulses, a method that Hoof and Patsch proposed and named as ''Pulse Sequence Analysis'' (PSA) [31]. This analysis generates graphical patterns or ''maps'' that identify different defects that are sources of PDs in insulation systems with a higher recognition rate than the PRPD patterns for some cases [33], [34]. A PSA pattern is usually constructed with the instantaneous voltage differences between consecutive pulses, the n-th and $(n-1)$-th PD, yielding a scatter plot Δu_n versus Δu_{n-1}. In the case of electrical trees produced at industrial frequencies, patterns that relate both the voltage and time between pulses, $\Delta u_n/\Delta t_n$, have been employed to produce distinct PSA patterns for this type of insulation defect [19], [33].

A more general approach is to consider the PD phenomenon as a nonlinear dynamic process, and thus, to study it using the mathematical approach of nonlinear time series analysis (NLTSA) and chaos theory in order to characterize the PD behaviour and its sequence of discharges [29], [30]. NLTSA tools have been used in electrical treeing to analyze time series of PD and to describe the growth through nonlinear parameters [4], [11], [20], [35], [36]. In this approach, a similar type of graphical representation can be plotted, normally called ''state-space trajectory'' or ''projection'' [29]. On the other hand, the most used nonlinear parameter for characterization is the correlation dimension [20], [35], [36].

In this work electrical treeing phenomenon is studied based on the analysis of time series of PD measurements: instantaneous applied voltage and PD amplitude (apparent charge) of PD pulses. The study mainly focuses on trees grown at VLF excitation and the main aim is to compare two PD analysis techniques: PSA plots, a more established method, with projection plots obtained using NLTSA techniques, a more recent approach in PD analysis. In addition, electrical tree growth at VLF excitation is characterized in terms of tree shape and the non-linear parameter of correlation dimension.

II. METHODOLOGY

Fig. 1 shows the methodology flow chart followed in this investigation. The experimental and analytical methods are explained in the followings subsections.

A. EXPERIMENTAL SETUP

The samples consisted of the conventional needle-to-plane arrangement with a gap distance of ∼2 mm between the needle tip and the ground plane, as shown in Fig. 2a. The needle electrode consisted of a hypodermic needle Terumo, with an approximate minimum curvature radius of 3 μm [37]. The samples were made of epoxy resin (Mepox - 1125/L, a DGEBA type of transparent resin), cured in a chamber at 25 ° C for 24 hours and post-cured at 50 ° C for 15 hours. An incipient electrical tree was created in each sample by applying 12-16 kV 50 Hz voltage, until the incipient tree was

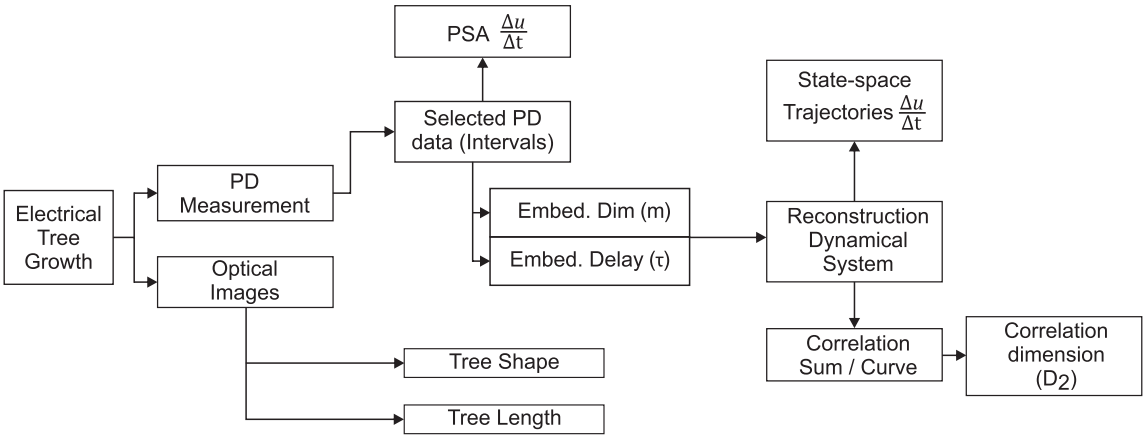

FIGURE 1. Flow chart of the method used for analysis of PD in electrical trees.

optically visible, and then observed under a microscope to verify the initiation of a tree in the sample. The transparent nature of the epoxy resin used facilitated the visualization of electrical trees inside the material.

For the electrical tree growth experiment, the balanced-type test circuit, according to the IEC 60270 standard [6], was implemented as shown in Fig. 2b. In the balanced test circuit, N_1 corresponded to a round electrode, which had negligible PD activity, and N_2 is the treeing sample (Fig. 2b). Thus, the main feature of the circuit was to achieve a better sensitivity of the PD measurements on the needle-plane test samples.

The voltage source of the circuit for the VLF experiments was a Baur Frida device and for the industrial frequency experiments the source was a testing transformer with a variac. In Fig. 2b, SC was the subtracting circuit where the PD pulses were sent to the acquisition system. A commercial PD detection system (Omicron MPD 600) was used for PD measurement and acquisition of time series, obtaining the PD amplitude q_n, time of occurrence t_n, and phase angle ϕ_n of each discharge during the entire experiment. The integration frequency was set to 250 $\pm$ 150 kHz, and the minimum adjustable time between recorded consecutive pulses (pulse-to-pulse resolution) was 6.25 μs. The voltage was measured using a voltage divider (V_m in Fig. 2b) and recorded using Omicron MPD 600. The high voltage resistor R of Fig. 2b was connected to reduce disturbances coming from the high voltage source and to limit the current in case of electrical tree breakdown. The minimum magnitude of PD amplitude was set at 2 pC for recording, however, the analysis was carried out with a threshold between 10 to 15 pC, since the background noise was not constant for all the experiments.

Tree growth was monitored with an optical camera connected to a personal computer for subsequent analysis. During the tests, the samples were immersed in a silicone oil cell to prevent unwanted external discharges on the surface of the test samples. The samples were subjected to high voltages of 12, 14 and 16 kV, using VLF 0.1 Hz and industrial frequency of 50 Hz, until electrical breakdown occured. These test voltages were selected due to experimental reasons: tree growth rate for voltages below 12 kV was too low, and unwanted discharges such as corona from connections and surface discharges from test sample could emerge for voltages above 16 kV. Several experiments were carried out, but only six tests were chosen for analysis, three under VLF and three under 50 Hz. Table 1 summarizes the conditions for these tests, and the resulting time to breakdown of each selected sample.

TABLE 1. Electrical tree samples grown at very low frequency 0.1 Hz and industrial frequency 50 Hz.

Sample name	Voltage (kV)	Freq. (Hz)
12-0.1	12	0.1
14-0.1	14	0.1
16-0.1	16	0.1
12-50	12	50
14-50	14	50
16-50	16	50

B. SELECTION OF DATA FOR ANALYSIS

Partial discharges were recorded during the entire experiment of tree growth, therefore, a large amount of data was collected, which imposed computational restrictions to the analysis. However, this was not a limitation, due to the use of enough windows or intervals for the study of the parameters' evolution during tree growth. Thus, several intervals of analysis were selected from the entire time series following a similar methodology previously used [11], [36]. Each interval was selected to have at least 10,000 PD events and at least 1,000 and 10 seconds for 0.1 and 50 Hz experiments respectively. The first analysis interval was set to start after three minutes from the beginning of the test to reach a more stable PD activity. The last interval was set to finish at least five minutes before the breakdown, whereas the distance between intervals depends on the duration of each test.

C. PD ANALYSIS TECHNIQUES

1) PULSE SEQUENCE ANALYSIS (PSA)

When partial discharge occurs in solid or liquid dielectrics, the externally applied voltage does not only relate with the

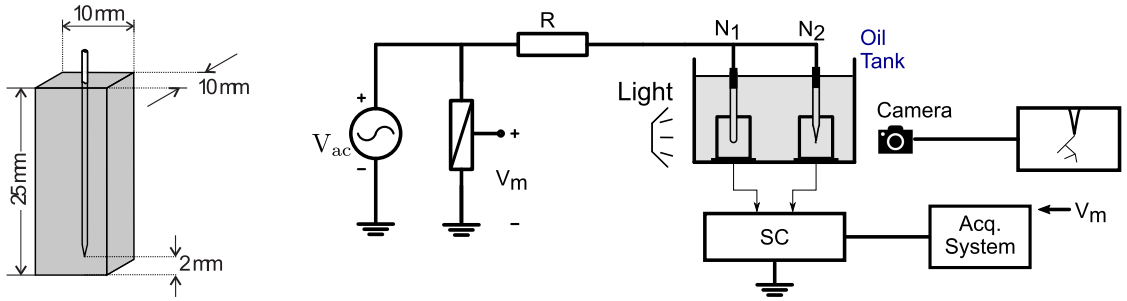

(a) Needle-plane geometry of epoxy resin samples.

(b) Circuit for PD measurement and tree growth monitoring.

FIGURE 2. Experimental diagrams.

local electric field at the cavity, which produces the discharge. The variation of the local electrical field is influenced by physical phenomena such as charge transportation to the bulk and surface conductivity, among others [38], [39]; however, it is not possible to measure these physical phenomena directly and easily. Thus, pulse sequence analysis (PSA) was used to obtain information about the changes of the local electric field from variables that could be measured externally [31]. In this method, each PD pulse could be represented by its charge amplitude q_n, time of occurrence t_n, the voltage of occurrence u_n or phase of occurrence φ_n. This information about the PD sequence is processed and plotted, resulting in several patterns that could be analyzed either qualitatively [19], [40], [41] or quantitatively [32]–[34].

In this work we use the parameters u_n and t_n to calculate $\Delta u_n/\Delta t_n$ for PSA. The construction of PSA plots from the PD pulse sequence is illustrated in Fig. 3. A qualitative analysis approach was followed through the comparison of PSA plots with typical patterns, and their changes with the electrical tree growth.

To calculate the required parameters, the sampled applied voltage must be interpolated to obtain its value at the instant when the PDs are produced. Using these interpolated values the quotient between voltage difference and the time difference is calculated using (1):

$$\frac{\Delta u_n}{\Delta t_n} = (u_n - u_{n-1})/(t_n - t_{n-1}) \cdot 1/(V_b \cdot f_b) \qquad (1)$$

Note that (1) is normalized by the peak test voltage V_b and the test frequency f_b to avoid the differences coming from the magnitude of the voltage or the frequency. Usually, the parameter Δu_n is considered as proportional to the local electric field changes at the discharge site [31]; therefore, Δu_n could give information about changes in the spatial distribution of charge and its dynamics. The parameter $\Delta u_n/\Delta t_n$ could be used instead of Δu_n to emphasize pulse sequence with short time intervals between them; an idea that is particularly useful when solids are involved, because the nature of discharges in this situation produces patterns with very discernible clusters [33]. During electrical treeing, the patterns generated are like the one shown in Fig. 4a, where six

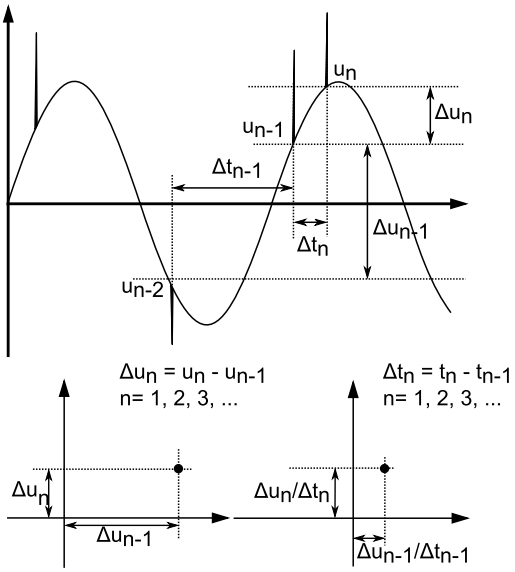

FIGURE 3. Transformation of PD pulse sequence into $\Delta u_n(u_{n-1})$ and $\frac{\Delta u_n}{\Delta t_n}(\frac{\Delta u_{n-1}}{\Delta t_{n-1}})$ [31].

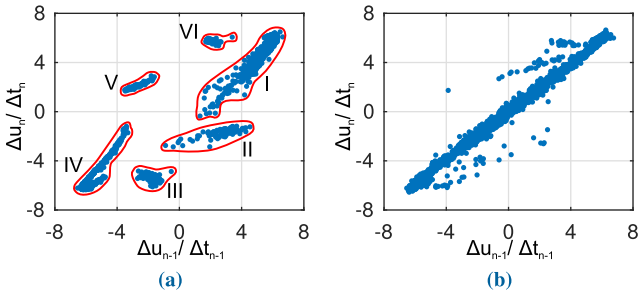

FIGURE 4. Examples of $\Delta u_n/\Delta t_n$ PSA plots for electrical treeing. (a) Sample 12-0.1, interval 5. (b) Sample 14-0.1, interval 10, near to breakdown.

different clusters are observed; although, during the runaway stage, patterns as the presented in Fig. 4b have been observed [19], [40], [41].

2) NONLINEAR TIME SERIES ANALYSIS

Electrical trees are a complex physical phenomenon that can be analyzed using the theory of nonlinear dynamic systems

through the tools provided by nonlinear time series analysis (NLTSA) [4], [5]. If a dielectric subjected to degradation by electrical treeing is represented by a nonlinear dynamic system, it can be mathematically described by a set of differential (difference) equations, (2), where $\mathbf{y} \in \mathbf{Y} \subset \mathbb{R}^n$ is the state vector of the system [35].

$$\begin{aligned} \dot{\mathbf{y}} &= \mathbf{F}(\mathbf{y}) \\ \mathbf{y}(0) &= \mathbf{y}_0 \end{aligned} \tag{2}$$

Typically, in electrical treeing process many of the states are unknown [5] and, therefore, the exact mathematical description is also unknown. However, as in many experimental settings, it is possible to measure one quantity of interest and describe the underlying dynamic system. This is possible by using Taken's embedding method, the "delay coordinate embedding" [42], which allows to reconstruct the state space of a dynamical system from the measurement of only one observable variable of the system. For the reconstruction is necessary to estimate two parameters: the embedding dimension m and the embedding delay τ; then, if $\{x_n\}_{n=1,2,3,\ldots,N}$ is the measured observable variable, the set of points described in (3) is the reconstruction of the state space:

$$\mathbf{x}_n = \left(x_n,\ x_{n+\tau},\ x_{n+2\tau},\ \ldots,\ x_{n+(m-1)\tau}\right) \quad \text{for } n = 1, 2, \ldots, N-(m-1)\tau \tag{3}$$

The false nearest neighborhood method [43], which aims to find the minimal embedding dimension required to resolve the geometrical structure in the state space of the underlying dynamic system, was used for the estimation of m. The estimation of τ was made through the mutual information method [44]. In this method, the mutual information is calculated for different embedding delays. The value of embedding delay that corresponds to the first minimum of the mutual information is taken as τ for reconstruction. It can be interpreted that $x(t+\tau)$ adds the largest amount of information to that already known from $x(t)$ without completely losing information of the correlation between them [45].

In nonlinear dynamic systems, one commonly used method for analyzing the system dynamics is through the phase-space representation, i.e. state-space trajectories, which is a graphical description where the system variables are plotted against each other [46]. Using Taken's reconstruction method, from the time series of one observable variable, the state-space trajectory can be projected in two dimensions using two components of the reconstructed vector x_n, and so the trajectory can be graphically represented. These projections resemble patterns as in the case of PSA plots. This is the reason why in this article both graphical representations are compared: PSA plots and projections of the state-space trajectories from NLTSA. The time series of $\Delta u_n/\Delta t_n$ were used in the comparison of both representations. This type of time series was previously used in PSA plots to display properties in the case of electrical trees [19], [33]. It is worth noting that PSA plots can be seen as the particular case of 2D projections (NLTSA) with delay τ equals to 1, however, the PSA tool was developed from a physical reasoning rather than derived from the theory of nonlinear dynamic systems [32].

The dynamic characteristics of the system can be analyzed through some parameters, being one of them the correlation dimension D_2. This parameter allows the estimation of the fractal dimension of a geometrical object that represents a reconstructed state space [4], [5]. To introduce the concept of D_2, consider a reconstructed state space whose trajectory is described by a set of points $\mathbf{x}_n \in \mathbf{X} \subset \mathbb{R}^m$. If this set describes a long term trajectory that has evolved to a bounded region of the space, it establishes an asymptotic limit represented by a bounded trajectory; this limit is usually called an *attractor*. The geometry of the attractor could be a very complex object with fractal properties; in such a case, we referred to that as a *strange attractor* [36]. To quantify the fractal properties of this attractor usually the correlation dimension is calculated [47]. In order to do it, it is first necessary to calculate the correlation sum by using (4):

$$C_2(\epsilon) = \frac{2}{N(N-1)} \sum_{i=1}^{N} \sum_{j=i+1}^{N} \Theta(\epsilon - \left\|\mathbf{x}_i - \mathbf{x}_j\right\|) \tag{4}$$

In (4) $\Theta()$ is the Heaviside function and N is the total amount of points. The number $C_2(\epsilon)$ can be interpreted as an average distribution of points of the set $\{\mathbf{x}_i\}$ in small balls of radius ϵ [36]. Once C_2 is calculated, the correlation dimension is estimated by finding a range of ϵ where

$$\ln C(\epsilon) \approx D_2 \cdot \ln(\epsilon) + constant. \tag{5}$$

This range is usually called as the *scaling range* [46].

At this point, it is important to remark that the quantity that could be calculated automatically is the correlation sum $C(\epsilon)$. The correlation dimension D_2 may be assigned only after a careful interpretation of the curves of $C(\epsilon)$ and, if it is possible, using any other information available [46].

An example of correlation sum curve is shown in Fig. 5a. The blue curve corresponds to $\ln C(\epsilon)$, whereas the red curve is a straight line that is fitted to the "scaling range" of $\ln C(\epsilon)$. For small values of ϵ the curve $\ln C(\epsilon)$ shows a discrete behavior, that could be a consequence of the discretization error (see Fig. 5a). Once this curve shows a "continuous" behavior, a scaling range is searched starting from the small ϵ. To obtain a better estimation for D_2 is recommended to verify that D_2 saturates with increasing embedding dimension m [46]. An example of this analysis using experimental data of PD in electrical trees is presented in Fig. 5b, where it is possible to observe that D_2 saturates at ≈ 4.75. The range of convergence for this data is $6 \leq m \leq 9$, which is in concordance with the value of m estimated through false nearest neighborhood method that is equal to 7; in this sense, this last value provides a guideline about when D_2 saturates and, thus, the necessary value of m to calculate C_2.

In this work, the correlation dimension D_2 for the times series of PD amplitude (apparent charge) q_n is calculated for the 0.1 Hz tests under analysis. The analysis of q_n through

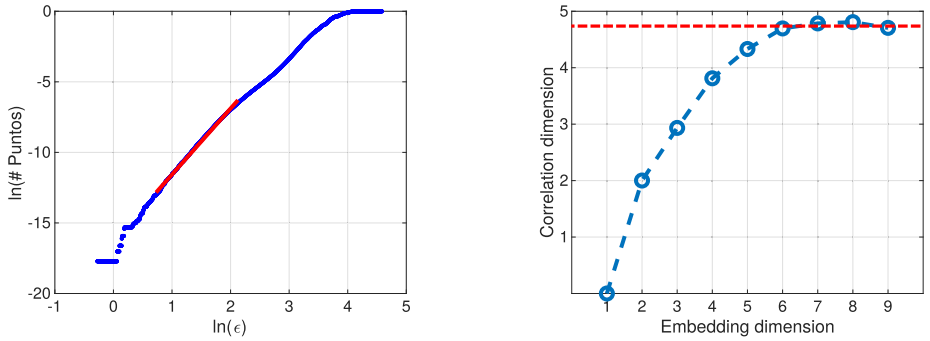

(a) Calculation of D_2 from C_2-curve.

(b) Saturation of D_2 with the increasing m.

FIGURE 5. Example of calculation of correlation dimension D_2.

NLTSA tools is usually associated with the charge dynamics [20], [35], so it could reveal information about changes occurred in electrical tree.

III. RESULTS AND ANALYSIS

Despite the fact that electrical treeing experiments of both 50 Hz and VLF were carried out (see Table 1), the results presented here are mainly focused on VLF excitation, since it is the aim of this work. This analysis focus was chosen due to the main novelty is the analysis of electrical trees grown at VLF using NLTSA tools, and the graphical comparison with PSA plots.

A. TIME SERIES OF PD AND ELECTRICAL TREE STRUCTURE

The experimental results for the samples aged at 12, 14 and 16 kV for VLF excitation are respectively shown in Fig. 6a, 6b and Fig. 6c: to the left, the time series of PD amplitudes and normalized tree length, calculated based on the tree images, and to the right, images of the tree growth at different stages of the degradation. For the following analysis, the intervals of the PD amplitudes time series considered, as defined in Section II-B, are highlighted in red. In those intervals, the electrical tree length was measured, and we considered this parameter as the main representation of the degradation by treeing in the dielectric. Tree length was measured as the furthest tree extent from the needle tip in direction to the ground plane, and it was normalized by the length of the first branch that reached the ground electrode. A normalized length equal to one thus indicates that the electrical tree has crossed the insulation, bridging the electrodes.

In the three samples shown in Fig. 6, the time series of PD amplitudes had an increasing value behaviour in each case, starting with low values and then reaching higher values near the end of the experiment. A period with negligible PD activity was observed at the beginning of the electrical tree growth of samples aged at 12 and 14 kV, near to the detection threshold. In the case of 16 kV, this period was almost non existent. Branch-type of electrical trees were observed in the test samples as shown in Fig. 6, although, qualitatively, the density of tree structures was different. The electrical tree at 12 kV is characterized by a major trunk like some DC trees [10], [48]. The electrical tree at 14 kV evolved similar to a filamentary structure, i.e. less branch-density than the other samples, having almost an imperceptible structure at the beginning (near to the tip of the needle). Considering this observation, the connection of partial discharge phenomena and electrical trees [49] could explain the lower values of PD amplitude obtained in the sample at 14 kV in comparison with the other samples. In contrast, the electrical tree aged at 16 kV had a denser structure and, consequently, a higher value PD activity, as expected: more 'bushy' type electrical trees are associated with larger PD amplitude [36], [50]. Pictures of the resulting electrical trees prior breakdown for 50 Hz excitation frequency are shown in Fig. 7. It is observed that the electrical trees under 50 Hz frequency tended to have a higher number of branches with a denser tree structure in comparison to the 0.1 Hz trees (Fig. 6), which is in agreement to [9], [36].

The time to breakdown (TTB) was observed to decrease in terms of the voltage level applied, for both VLF and 50 Hz excitations, as depicted in Fig. 8. The TTB trend at both frequencies was found to be similar, and TTB for 0.1 Hz tests were in average 50 times larger than the TTB of 50 Hz samples. In terms of the evolution of the electrical tree length values, the samples aged at 12 and 14 kV had a similar trend (see Fig. 6), meanwhile the sample at 16 kV showed a trend that resembles a curve of the exponential form.

B. $\Delta u/\Delta t$ plots

The results of the pulse sequence analysis (PSA) patterns and 2D projections from the non-linear time series analysis (NLTSA) are shown in Fig. 9. Each sub-figure has two rows containing the plots generated for intervals 1, 4, 7 and 10: the top row corresponds to the PSA $\Delta u_n/\Delta t_n$ patterns and the bottom row corresponds to the 2D-projections of the NLTSA. Note that the quantities in Fig. 9 were normalized as explained in Section II-C1.

Additionally, in Table 2 are shown the calculated embedding delays τ required to make the 2D projections using NLTSA (see Section II-C2 for their calculation), and the

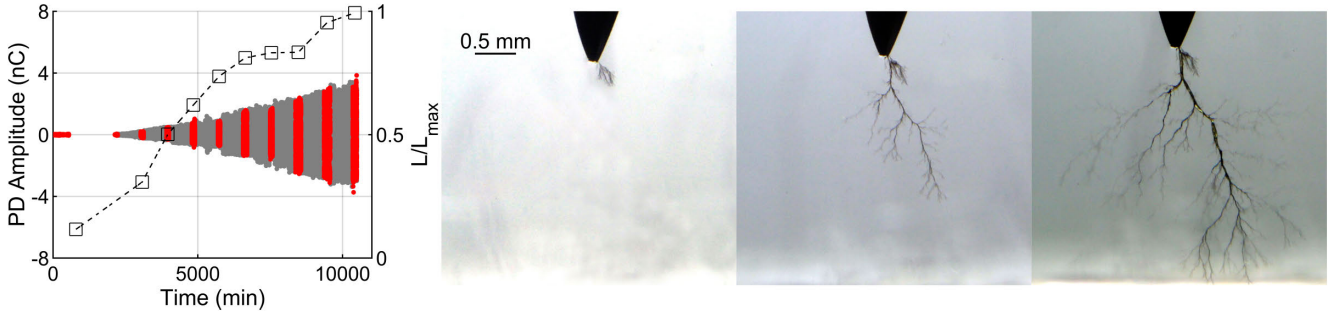

(a) 12-0.1

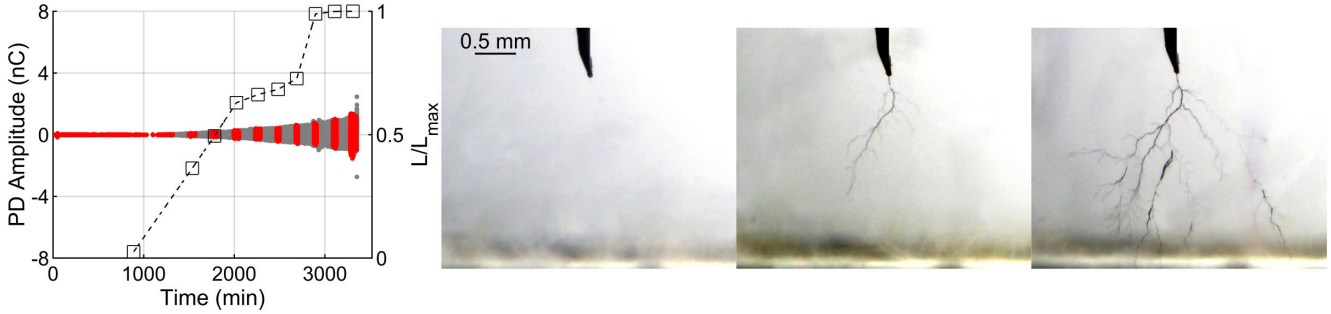

(b) 14-0.1

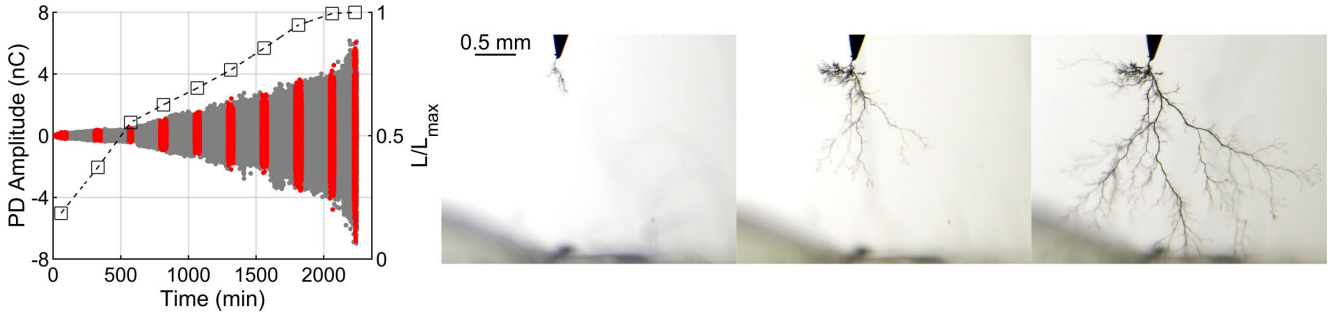

(c) 16-0.1

FIGURE 6. PD time series and shapes for electrical trees growth under VLF 0.1 Hz excitation.

normalized electrical tree lengths corresponding to each interval of analysis (stage of tree growth). The values of the intervals shown in Fig. 6 are highlighted. Recall that the PSA patterns can be thought as a reconstruction of the space using a $\tau = 1$, i.e. a relation of two consecutive pulses. In contrast, the 2D projections can establish an analogous relationship between two non-consecutive values of the time series, but separated by τ values between them (see Table 2). This representation was thought as an optimal embedding delay value in terms of the mutual information algorithm [44].

A notorious difference was observed between PSA plots and NLTSA projections. At the beginning of the electrical tree growth (interval 1), both PSA and NLTSA produced plots displaying clusters that were different to the respective following intervals. It had been reported that diverse phenomena influence the initial electrical tree process [33], [51] and both analyses were found to be sensible at this initial part. In the middle stages of the degradation, intervals 4 and 7 in Fig. 9, the PSA patterns obtained were similar to the ones reported in other studies at industrial frequency [19], [41]; this could be a sign that the underlying tree-growth mechanisms are similar under both frequencies. On the other hand, the NLTSA projections formed a higher number of clusters with an overall different shape with respect to the PSA patterns. Particularly, the clusters were distributed in a different manner [46], [52]. In the final stage, interval 10, the PSA patterns of the 12-0.1 and 14-0.1 samples varied slightly in comparison to the middle stages, whereas the 16-0.1 sample showed a behaviour observed in electrical tree runaway stage, with a main cluster aligned to the 45° line. Overall, the NLTSA results showed that there was not a complete loss of correlation between values of times series of PD amplitude (apparent charge).

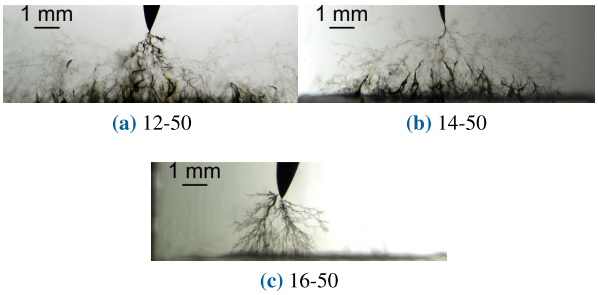

(a) 12-50 (b) 14-50

(c) 16-50

FIGURE 7. Images of electrical trees prior breakdown for samples under 50 Hz excitation.

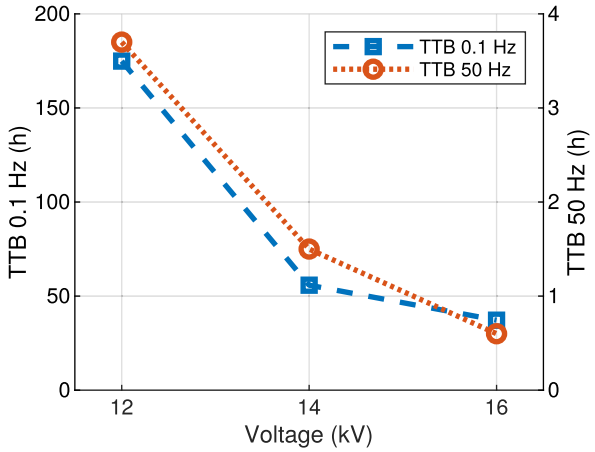

FIGURE 8. Time to breakdown (TTB) for 0.1 and 50 Hz samples.

TABLE 2. Embedding delay and normalized tree length for 0.1 Hz tests.

Interval	12-0.1		14-0.1		16-0.1	
	τ	L/L_{max}	τ	L/L_{max}	τ	L/L_{max}
1	**6**	**0.11**	**6**	**0.03**	**6**	**0.18**
2	5	0.30	8	0.35	12	0.37
3	6	0.49	8	0.47	14	0.55
4	**5**	**0.61**	**9**	**0.61**	11	**0.62**
5	6	0.73	9	0.64	13	0.68
6	5	0.80	13	0.66	13	0.76
7	**6**	**0.83**	**11**	**0.70**	**12**	**0.84**
8	2	0.83	19	0.99	9	0.94
9	3	0.99	12	1.00	11	0.99
10	**3**	**1.00**	**9**	**1.00**	**10**	**1.00**

A complete loss of correlation would have resulted in a random distribution of values in the phase space [46], [52]. Considering the patterns and projections obtained (Fig. 9), only the sample aged at 16 kV showed the signs of electrical treeing runaway in both analyses (PSA and NLTSA), and thus, these techniques could serve for the task of identifying the imminent breakdown, i.e. predicting the dielectric failure. At middle stages, using either of these analyses, no clear signs of the evolution/trend of clusters were found to be useful in predicting failure.

C. CORRELATION DIMENSION CALCULATION

The correlation dimension D_2 for the selected time series of PD amplitude, see Fig. 6, was calculated and it is presented as function of the normalized tree length in Fig. 10.

The variation range of D_2 was in the same order of magnitude for all the samples analyzed, although there was no unique tendency in the evolution of this parameter. In samples 12-0.1 and 16-0.1, the value of D_2 increased until $L/L_{max} \approx 0.6$ (interval 4), however, this behavior was not observed in 14-0.1 sample. After interval 4, all the samples analyzed showed a decrease in the D_2 value and was observed to occur when the normalized tree length was between 0.65 and 0.7 approximately. In 12-0.1 and 14-0.1 samples, this behaviour coincided with a slower rate of change in the normalized tree length, see Fig. 6a and Fig. 6b. Over 0.7 of normalized tree length, the behaviour of D_2 values was variable in all the cases. Note that near to the final stage of the electrical tree growth, the samples (especially 14-0.1 and 16-0.1 samples) showed a sharp increase in D_2 value.

IV. DISCUSSION

A. PD TIME SERIES AND ELECTRICAL TREE GROWTH

Partial discharge time series obtained from the experiments (Fig. 6) had a growing trend during the entire tree growth. In most of the reports about electrical treeing at industrial frequency, different trends had been found, including periods when negligible PD activity was measured. [1], [20], [53]. The difference between VLF and 50 Hz in the behaviour of times series of PD amplitude could be related with the charge relaxation or charge transport phenomena in PDs [32], [38], [39], [54]: with a lower excitation frequency the electric charge has more time for recombination, which reduces the possibilities of discharge extinction due to deposition of cations in sidewalls of the tree [1]. Furthermore, under 0.1 Hz excitation, the increase of PD amplitude as the size of the electrical tree increases, could be a sign that the conductivity of the tree channels is low [50], [51].

Fig. 6 qualitatively showed that the tree growth at 0.1 Hz and 16 kV had a slightly denser structure than at 12 and 14 kV. This observation is consistent with the experience under 50 Hz: increasing the voltage produces an increase in tree branch-density [50]. Despite that, electrical tree shapes under VLF excitation were notoriously more 'branchy' than tree structures under 50 Hz (compare Fig. 6 and 7). This branch-type of the electrical trees observed at VLF can be understood in terms of the discharge avalanche model (DAM) developed by Dissado *et al.* [4]. In such model, the frequency of the excitation source influences the available time for the space charge transport in the dielectric according to $\frac{1}{2f}$. Then, as the electric charge has more time for relaxation, the Poisson electric field component of the total electric field decreases, and thus the electric field is mainly dominated by its Laplacian component. In turn, this effect could give rise to fewer bifurcations in the tree structure and could explain the difference between 0.1 and 50 Hz electrical trees [4].

B. PSA PLOTS AND NLTSA 2D PROJECTIONS

This work aimed the comparison of PSA plots and 2D projections of the state-space trajectories of the reconstructed

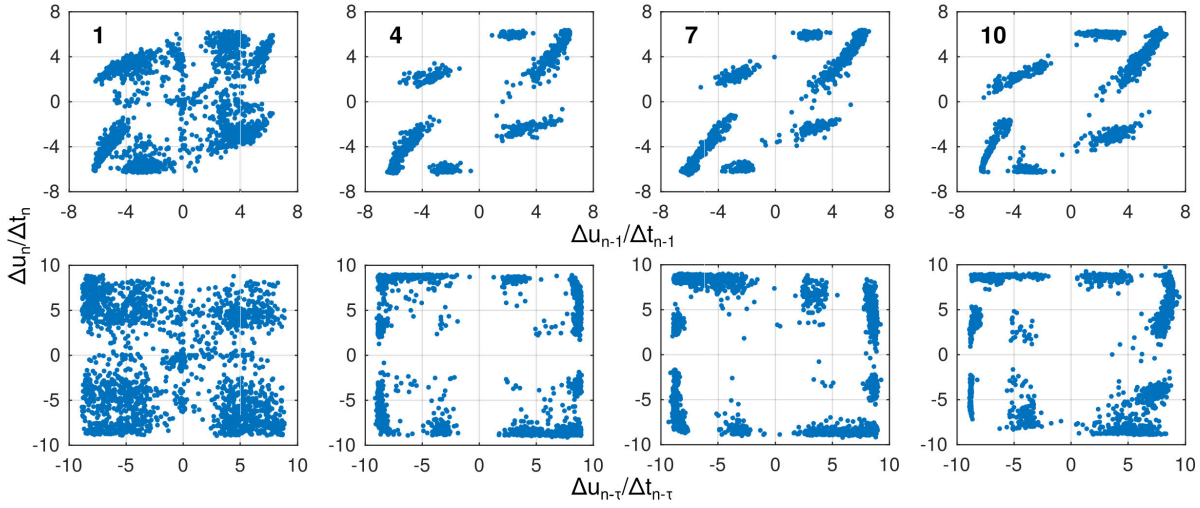

(a) 12-0.1

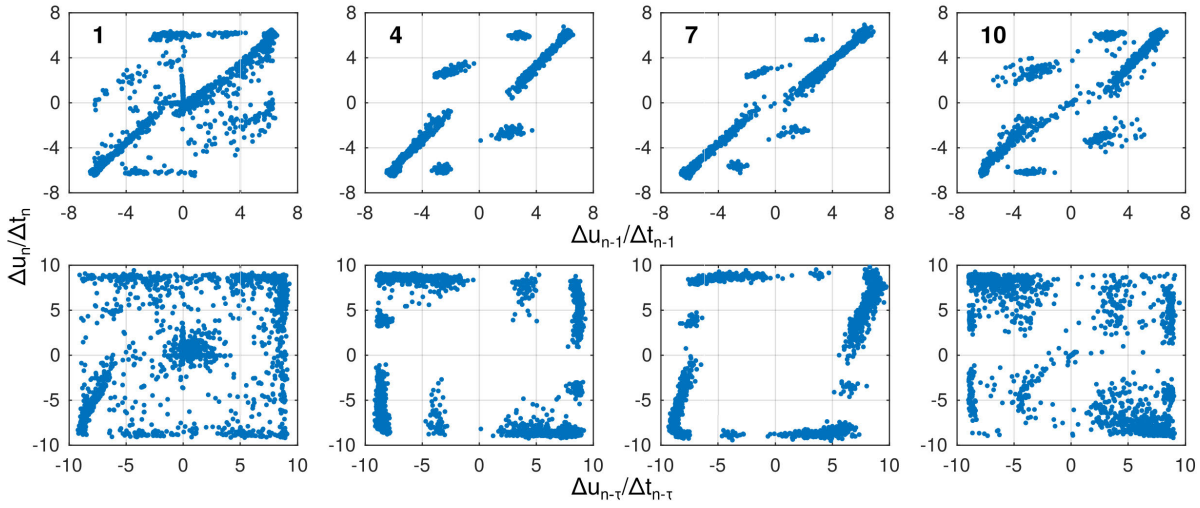

(b) 14-0.1

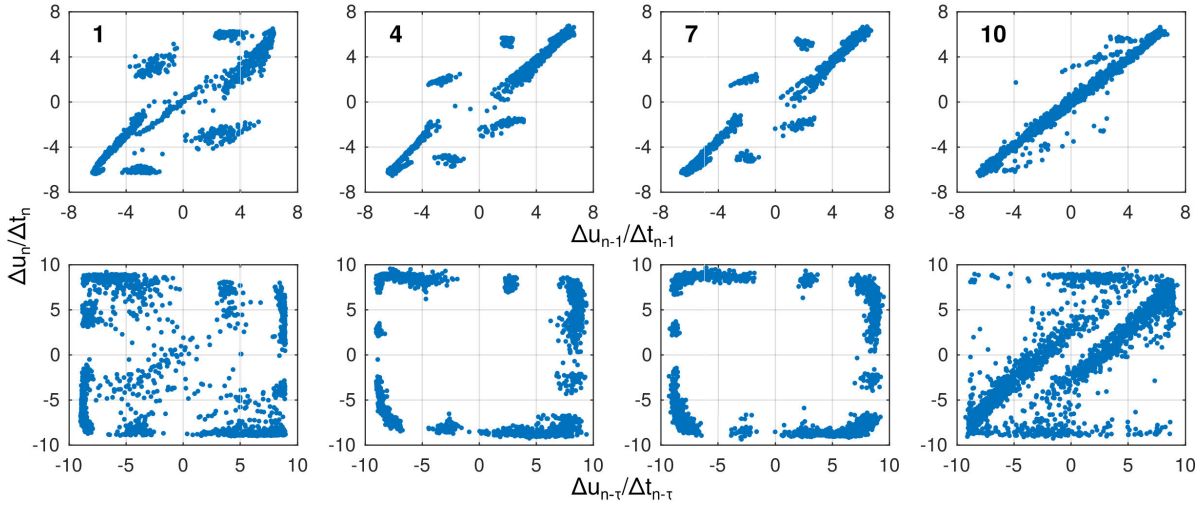

(c) 16-0.1

FIGURE 9. Representative PD patterns of $\Delta u_n/\Delta t_n$ PSA plots and 2D projections for 0.1 Hz tests. In each sub-figure: top row, PSA plots, and bottom row: NLTSA 2D projection plots.

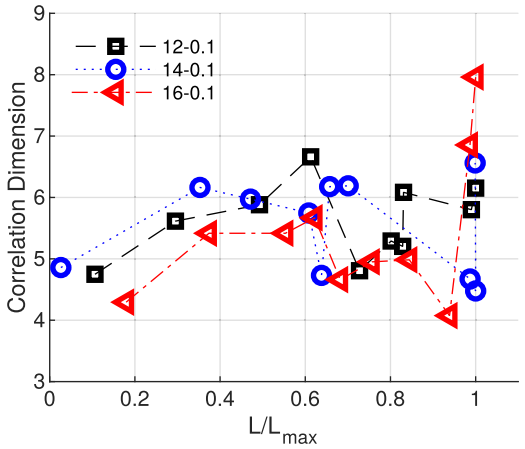

FIGURE 10. Correlation dimension as function of tree length.

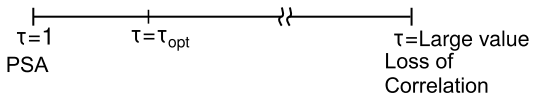

FIGURE 11. Interpretation of τ values.

dynamic system (NLTSA approach), because despite the fact that they have different theoretical background, they are similar in their generation and display. As commented in previous sections, PSA plots can be seen as the graphical description of the reconstruction of the space using an embedding dimension $m = 2$ and embedding delay $\tau = 1$, i.e. a particular case of the more general approach used in the reconstruction of nonlinear dynamic systems, where the parameters m and τ are obtained from algorithms of optimization.

The situation can be analyzed considering Fig. 11, which describes the meaning of possible values for τ. On the left end $\tau = 1$, i.e. the case of PSA plots. In this case, the relation between PD measurements is only with consecutive PDs, resulting that the points of the maps tended to stay in the 45° line, since this delay was not able to adequately disclose the dynamic of the reconstructed system. On the other end, if a large value is chosen for τ, it would be a loss of correlation bewteen the points, resulting in a kind of random distribution of the points in the reconstructed phase-space [45], [46], [52]. Between both ends, an optimum τ can be calculated from the mutual information algorithm, a value that produces projections with more disperse points in the space, and so delivering more information than PSA and displaying characteristic patterns related to the state of the underlying dynamic system. In other words, if we assume that the measured variable, the PD amplitude, is part of a more complex system, i.e. having a higher number of variables both unknown and not measured, when we use PSA approach ($m = 2, \tau = 1$) the attractor set in this higher dimension state space showed an attractor that tended to be aligned with the identity line, e.g. see Fig. 9b interval 7. Those PSA values of embedding dimension and delay are insufficient to describe the entire chaotic structure of the attractor. In contrast, the 2D projections using the NLTSA approach generated more disperse patterns (compare PSA plot and 2D projection of interval 7 in Fig. 9b). In general, NLTSA 2D projections generated a higher number of clusters with various locations compared to PSA plots. The occurrence of other clusters can also be interpreted as a more detailed description of attractors present in this complex system, that cannot be observed with the PSA analysis parameters m and τ.

In terms of electrical tree growth, both analyses seemed insufficient to describe the process of electrical tree growth. Although PSA plots and NLTSA 2D projections presented patterns normally associated with electrical tree PD activity, a distinctive evolution that could be useful to characterize the ageing process, specially the last interval closer to the breakdown, was not obtained, except for the well known electrical tree runaway analogous to the industrial frequency excitation [19], [41]. PSA has been found insufficient for analyzing the electrical tree phenomena at industrial frequency in other reports [40], and in this work, at very low frequency excitation, both sequence analyses (PSA and NLTSA plots) cannot determine the stage of tree growth.

C. CORRELATION DIMENSION

The correlation dimension parameter D_2 has been used to characterize the geometrical structure of electrical trees [4]. Different behavior of D_2 with the progression of electrical trees have been reported [11], [20], [35]. The trend found in this work under VLF excitation, see Fig. 10, was not similar to these previous reports. The findings in this work showed a distinctive behavior in terms of the electrical tree length: a progressive evolution until 0.6 p.u. (normalized tree length), then an abrupt decrease approximately between 0.6-0.7 p.u. and finally a sharp rise near the breakdown. It is not clear if this behaviour can be used to infer the dielectric breakdown in terms of the analysis of the correlation dimension in electrical treeing under VLF excitation, but it is remarked that this behaviour is definitely different to the reported on studies carried out at industrial frequencies.

V. CONCLUSION

In this work, electrical tree growth in epoxy resin samples aged at VLF was studied using two sequence analyses approaches: PSA and NLTSA from the nonlinear dynamic system theory.

The shape of the trees obtained was branch type, with fewer branches than the test samples aged at industrial frequency. The time series of the PD amplitude showed a steady increase in magnitude as the electrical tree grew. This observed behavior can be a distinctive characteristic of tree growth under VLF, compared to reports of tree growth under industrial frequency.

For this article, PSA was considered as a particular case of the graphical representation of state-space trajectories projected in 2D, using NLTSA tools. In contrast to PSA plots, NLTSA generated more clusters and distributed differently. From this, it was concluded that NLTSA can reveal the

structure of the dynamic system attractors with more detail than PSA. However, this mathematical interpretation is not necessarily better than PSA plots to assess the stage of growth of electrical trees.

Another method of analyzing nonlinear dynamics systems is through the evolution of characteristic parameters such as the correlation dimension D_2. For the VLF samples presented here, D_2 showed variation during tree growth, with a sharp increase in the final stage close to the breakdown. The authors consider that the results presented in this article broaden the way of analyzing the growth of electrical trees under VLF and confirm the need to continue evaluating and developing new tools in order to more accurately characterize the behavior of this degradation phenomenon.

REFERENCES

[1] L. A. Dissado and C. Fothergill, *Electrical Degradation and Breakdown in Polymers*, 1st ed. London, U.K.: Peter Peregrinus, 1992.

[2] J. H. Lawson and W. Vahlstrom, "Investigation of treeing in 15 and 22 KV polyethylene cables removed from service," in *Proc. Conf. Electr. Insul. Dielectr. Phenomena (CEIDP)*, Oct. 1972, pp. 255–265.

[3] J. Lawson and W. Vahlstrom, "Investigation of insulation deterioration in 15 KV and 22 KV polyethylene cables removed from service—Part II," *IEEE Trans. Power App. Syst.*, vol. PAS-92, no. 2, pp. 824–835, Mar. 1973.

[4] L. A. Dissado, S. J. Dodd, J. V. Champion, P. I. Williams, and J. M. Alison, "Propagation of electrical tree structures in solid polymeric insulation," *IEEE Trans. Dielectr. Electr. Insul.*, vol. 4, no. 3, pp. 259–279, Jun. 1997.

[5] L. A. Dissado, "Understanding electrical trees in solids: From experiment to theory," *IEEE Trans. Dielectr. Electr. Insul.*, vol. 9, no. 4, pp. 483–497, Aug. 2002.

[6] *High-Voltage Test Techniques—Partial Discharge Measurements Techniques*, IEC Standard 60270, 2015.

[7] J. V. Champion, S. J. Dodd, and J. M. Alison, "The correlation between the partial discharge behaviour and the spatial and temporal development of electrical trees grown in an epoxy resin," *J. Phys. D, Appl. Phys.*, vol. 29, no. 10, pp. 2689–2695, Oct. 1996.

[8] S. J. Dodd, "A deterministic model for the growth of non-conducting electrical tree structures," *J. Phys. D, Appl. Phys.*, vol. 36, no. 2, pp. 129–141, Jan. 2003.

[9] E. Ildstad, K. Fauskanger, and J. Hølto, "Electrical treeing from needle implants in XLPE during very low frequency (VLF) voltage testing," in *Proc. IEEE Int. Conf. Solid Dielectr. (ICSD)*, Jun. 2013, pp. 800–803.

[10] I. Iddrissu, H. Zheng, and S. M. Rowland, "DC electrical tree growth in epoxy resin and the influence of the size of inceptive AC trees," *IEEE Trans. Dielectr. Electr. Insul.*, vol. 24, no. 3, pp. 1965–1972, Jun. 2017.

[11] R. Schurch, P. Donoso, J. Ardila-Rey, J. Montana, and A. Angulo, "Electrical tree growth under very low frequency (VLF) voltage excitation," in *Proc. IEEE Conf. Electr. Insul. Dielectr. Phenomena (CEIDP)*, Oct. 2018, pp. 427–430.

[12] M. Bao, X. Yin, and J. He, "Structure characteristics of electrical treeing in XLPE insulation under high frequencies," *Phys. B, Condens. Matter*, vol. 406, no. 14, pp. 2885–2890, Jul. 2011.

[13] G. Chen and C. Tham, "Electrical treeing characteristics in XLPE power cable insulation in frequency range between 20 and 500 Hz," *IEEE Trans. Dielectr. Electr. Insul.*, vol. 16, no. 1, pp. 179–188, Feb. 2009.

[14] F. De la Rosa, *Harmonics, Power Systems, and Smart Grids*, 2nd ed. Boca Raton, FL, USA: CRC Press, 2015.

[15] *IEEE Recommended Practice and Requirements for Harmonic Control in Electric Power Systems*, IEEE Standard 519, 2014.

[16] *IEEE Guide for Field Testing of Shielded Power Cable Systems Using Very Low Frequency (VLF) (Less Than 1 Hz)*, IEEE Standard 400.2, 2013.

[17] R. Schurch, J. Ardila-Rey, J. Montana, A. Angulo, S. M. Rowland, I. Iddrissu, and R. S. Bradley, "3D characterization of electrical tree structures," *IEEE Trans. Dielectr. Electr. Insul.*, vol. 26, no. 1, pp. 220–228, Feb. 2019.

[18] L. A. Dissado, "Deterministic chaos in breakdown. Does it occur and what can it tell us?" *IEEE Trans. Dielectr. Electr. Insul.*, vol. 9, no. 5, pp. 752–762, Oct. 2002.

[19] N. M. Chalashkanov, S. J. Dodd, L. A. Dissado, and J. C. Fothergill, "Pulse sequence analysis on PD data from electrical trees in flexible epoxy resins," in *Proc. Annu. Rep. Conf. Electr. Insul. Dielectr. Phenomena (CEIDP)*, Oct. 2011, pp. 776–779.

[20] X. Chen, Y. Xu, and X. Cao, "Nonlinear time series analysis of partial discharges in electrical trees of XLPE cable insulation samples," *IEEE Trans. Dielectr. Electr. Insul.*, vol. 21, no. 4, pp. 1455–1461, Aug. 2014.

[21] J. V. Champion and S. J. Dodd, "The effect of voltage and material age on the electrical tree growth and breakdown characteristics of epoxy resins," *J. Phys. D, Appl. Phys.*, vol. 28, no. 2, pp. 398–407, Feb. 1995.

[22] *IEEE Guide for Partial Discharge Testing of Shielded Power Cable Systems in a Field Environment*, IEEE Standard 400.3, 2006.

[23] *IEEE Recommended Practice for Insulation Testing of AC Electric Machinery With High Voltage at Very Low Frequency*, IEEE Standard 433, 2009.

[24] H. R. Gnerlich, "Field testing of HV power cables: Understanding VLF testing," *IEEE Elect. Insul. Mag.*, vol. 11, no. 5, pp. 13–16, Sep. 1995.

[25] G. Montanari, "Bringing an insulation to failure: The role of space charge," *IEEE Trans. Dielectr. Electr. Insul.*, vol. 18, no. 2, pp. 339–364, Apr. 2011.

[26] T. Dao, B. T. Phung, T. Blackburn, and H. V. P. Nguyen, "A comparative study of partial discharges under power and very low frequency voltage excitation," in *Proc. IEEE Conf. Electr. Insul. Dielectr. Phenomena (CEIDP)*, Oct. 2014, pp. 164–167.

[27] R. Schurch, S. Rowland, R. Bradley, and P. Withers, "Imaging and analysis techniques for electrical trees using X-ray computed tomography," *IEEE Trans. Dielectr. Electr. Insul.*, vol. 21, no. 1, pp. 53–63, Feb. 2014.

[28] S. M. Rowland, R. Schurch, M. Pattouras, and Q. Li, "Application of FEA to image-based models of electrical trees with uniform conductivity," *IEEE Trans. Dielectr. Electr. Insul.*, vol. 22, no. 3, pp. 1537–1546, Jun. 2015.

[29] T. Czaszejko and R. Schurch, "State-space embedding as a visualization method for mixed partial discharge activities," in *Proc. Annu. Rep. Conf. Electr. Insul. Dielectic Phenomena (CEIDP)*, West Lafayette, IN, USA, Oct. 2010, pp. 1–4.

[30] L. Petrov, P. Lewin, and T. Czaszejko, "On the applicability of nonlinear time series methods for partial discharge analysis," *IEEE Trans. Dielectr. Electr. Insul.*, vol. 21, no. 1, pp. 284–293, Feb. 2014.

[31] M. Hoof and R. Patsch, "Voltage-difference analysis, a tool for partial discharge source identification," in *Proc. Conf. Rec. IEEE Int. Symp. Electr. Insul.*, vol. 1, Jun. 1996, pp. 401–406.

[32] M. Hoof and R. Patsch, "A physical model, describing the nature of partial discharge pulse sequences," in *Proc. 5th Int. Conf. Properties Appl. Dielectr. Mater.*, vol. 1, 1997, pp. 283–286.

[33] R. Patsch and F. Berton, "Pulse sequence analysis—A diagnostic tool based on the physics behind partial discharges," *J. Phys. D, Appl. Phys.*, vol. 35, no. 1, pp. 25–32, Jan. 2002.

[34] N. H. Aziz, V. M. Catterson, S. M. Rowland, and S. Bahadoorsingh, "Analysis of partial discharge features as prognostic indicators of electrical treeing," *IEEE Trans. Dielectr. Electr. Insul.*, vol. 24, no. 1, pp. 129–136, Feb. 2017.

[35] L. Barbieri, A. Villa, and R. Malgesini, "A step forward in the characterization of the partial discharge phenomenon and the degradation of insulating materials through nonlinear analysis of time series," *IEEE Elect. Insul. Mag.*, vol. 28, no. 4, pp. 14–21, Jul. 2012.

[36] R. Schurch, P. Donoso, P. Aguirre, O. Cárdenas, M. Zuniga, and S. M. Rowland, "Electrical tree growth and partial discharges analyzed by fractal and correlation dimensions," in *Proc. IEEE Conf. Electr. Insul. Dielectr. Phenomenon (CEIDP)*, Oct. 2017, pp. 785–788.

[37] S. Bahadoorsingh and S. Rowland, "Investigating the impact of harmonics on the breakdown of epoxy resin through electrical tree growth," *IEEE Trans. Dielectr. Electr. Insul.*, vol. 17, no. 5, pp. 1576–1584, Oct. 2010.

[38] L. Niemeyer, "A generalized approach to partial discharge modeling," *IEEE Trans. Dielectr. Electr. Insul.*, vol. 2, no. 4, pp. 510–528, Aug. 1995.

[39] H. Illias, G. Chen, and P. L. Lewin, "Partial discharge behavior within a spherical cavity in a solid dielectric material as a function of frequency and amplitude of the applied voltage," *IEEE Trans. Dielectr. Electr. Insul.*, vol. 18, no. 2, pp. 432–443, Apr. 2011.

[40] N. M. Chalashkanov, S. J. Dodd, L. A. Dissado, and J. C. Fothergill, "A comparison between PSA plots of partial discharges in needle voids and electrical trees," in *Proc. IEEE Int. Conf. Dielectr. (ICD)*, Jul. 2016, pp. 476–479.

[41] R. Schurch, L. Orellana, P. Donoso, J. Ardila-Rey, and J. Montana, "Pulse waveform, phase-resolved and pulse sequence analysis of partial discharges during electrical tree growth in epoxy resin," in *Proc. Int. Symp. High Voltage Eng. (ISH)*, 2017. [Online]. Available: https://e-cigre.org/publication/ISH2017_522-pulse-waveform-phase-resolved-and-pulse-sequence-analysis-of-partial-discharges-during-electrical-tree-growth-in-epoxy-resin
[42] F. Takens, *Detecting Strange Attractors Turbulence*, vol. 898. Berlin, Germany: Springer, 1981.
[43] M. B. Kennel, R. Brown, and H. D. I. Abarbanel, "Determining embedding dimension for phase-space reconstruction using a geometrical construction," *Phys. Rev. A, Gen. Phys.*, vol. 45, no. 6, pp. 3403–3411, Mar. 1992.
[44] A. M. Fraser and H. L. Swinney, "Independent coordinates for strange attractors from mutual information," *Phys. Rev. A, Gen. Phys.*, vol. 33, no. 2, pp. 1134–1140, Feb. 1986.
[45] M. Perc, "Introducing nonlinear time series analysis in undergraduate courses," *Fizika A-Zagreb*, vol. 15, nos. 1–4, pp. 91–112, 2006.
[46] H. Kantz and T. Schreiber, *Nonlinear Time Series Analysis*, 2nd ed. Cambridge, U.K.: Cambridge Univ. Press, 2004.
[47] P. Grassberger and I. Procaccia, "Measuring the strangeness of strange attractors," *Phys. D, Nonlinear Phenomena*, vol. 9, nos. 1–2, pp. 189–208, Oct. 1983.
[48] M. Azizian Fard, M. E. Farrag, A. Reid, and F. Al-Naemi, "Electrical treeing in power cable insulation under harmonics superimposed on unfiltered HVDC voltages," *Energies*, vol. 12, no. 16, p. 3113, Aug. 2019.
[49] H. Zheng and S. M. Rowland, "Electrical treeing in a glassy epoxy resin—The filamentary tree and the PD tree," in *Proc. IEEE Conf. Electr. Insul. Dielectr. Phenomenon (CEIDP)*, Oct. 2017, pp. 765–768.
[50] J. V. Champion and S. J. Dodd, "Simulation of partial discharges in conducting and non-conducting electrical tree structures," *J. Phys. D, Appl. Phys.*, vol. 34, no. 8, pp. 1235–1242, Apr. 2001.
[51] Z. Lv, H. Zheng, S. Rowland, and S. Chen, "Estimating the partial discharge inception and extinction voltage in a non-conductive electrical tree," in *Proc. IEEE 2nd Int. Conf. Dielectr. (ICD)*, Jul. 2018, pp. 1–4.
[52] E. Bradley and H. Kantz, "Nonlinear time-series analysis revisited," *Chaos, Interdiscipl. J. Nonlinear Sci.*, vol. 25, no. 9, Sep. 2015, Art. no. 097610.
[53] I. Iddrissu, S. M. Rowland, H. Zheng, Z. Lv, and R. Schurch, "Electrical tree growth and partial discharge in epoxy resin under combined AC and DC voltage waveforms," *IEEE Trans. Dielectr. Electr. Insul.*, vol. 25, no. 6, pp. 2183–2190, Dec. 2018.
[54] R. Bodega, P. H. F. Morshuis, M. Lazzaroni, and F. J. Wester, "PD recurrence in cavities at different energizing methods," *IEEE Trans. Instrum. Meas.*, vol. 53, no. 2, pp. 251–258, Apr. 2004.

PABLO DONOSO was born in Talagante, Chile, in 1993. He received the B.Sc. degree in electrical engineering from Universidad Técnica Federico Santa María (UTFSM), Valparaíso, Chile, in 2016, where he is currently pursuing the M.S. degree in electrical engineering. In 2018, he began his thesis work about partial discharge in electrical trees under very low frequency excitation analysed through nonlinear time series methods at the High Voltage Laboratory, UTFSM. His research interests include electrical treeing, partial discharges, and time series analysis.

ROGER SCHURCH (Member, IEEE) received the degree in electrical engineering from Federico Santa María Technical University (UTFSM), Valparaíso, Chile, in 2006, and the Ph.D. degree from The University of Manchester, in 2014. He was a High Voltage Equipment Analyst at Transelec Transmission Company, before joining UTFSM, as a Lecturer, in 2008. He rejoined UTFSM as an Assistant Professor. His research interests include electrical trees and partial discharges, and insulation diagnostics of power system plant.

JORGE ARDILA-REY (Member, IEEE) was born in Santander, Colombia, in 1984. He received the B.Sc. degree in mechatronic engineering from the Universidad de Pamplona, Pamplona, Colombia, in 2007, the Specialist Officer degree in naval engineering from the Escuela Naval De Cadetes Almirante Padilla, Cartagena, Colombia, in 2008, and the M.Sc. and Ph.D. degrees in electrical engineering from the Universidad Carlos III de Madrid (UC3M), in 2012 and 2014, respectively.

He was an Automatic Control Engineer of ARC Almirante Padilla, from 2008 to 2010. From 2010 to 2014, he worked with the Department of Electrical Engineering and the High-Voltage Research and Tests Laboratory (LINEALT), UC3M. He is currently working as a Professor with the Department of Electrical Engineering, Universidad Técnica Federico Santa María, Santiago, Chile. His research interests include partial discharges, insulation systems diagnosis, and instrumentation and measurement techniques for high-frequency currents.

LUIS ORELLANA was born in San Fernando, Chile, in 1992. He received the B.S. and M.S. degrees in electrical engineering from Federico Santa María Technical University, in 2015 and 2019, respectively.

He has experience in studying the relationship between the electromagnetic burst and other diagnostics from dense plasma focus devices at the Plasma and Nuclear Fusion Laboratory, Chilean Nuclear Energy Commission. His research interests include high-power pulse technology, applied plasma physics, and signal analysis.